



Article

A Systematic Study and Potential Limitations of Proton-ELISA Platform for α -Synuclein Antigen Detection

Chia-Ming Yang^{1,2,3,4,5,6,7} , Jia-Yuan Chang¹, Min-Yi Chen¹ and Chao-Sung Lai^{1,3,6,7,8,*} 

- ¹ Department of Electronic Engineering, Chang Gung University, Taoyuan 333, Taiwan; cmyang@mail.cgu.edu.tw (C.-M.Y.); d0827110@cgu.edu.tw (J.-Y.C.); monica0213@cgu.edu.tw (M.-Y.C.)
- ² Institute of Electro-Optical Engineering, Chang Gung University, Taoyuan 333, Taiwan
- ³ Biosensor Group, Biomedical Engineering Research Center, Chang Gung University, Taoyuan 333, Taiwan
- ⁴ Department of General Surgery, Chang Gung Memorial Hospital, Linkou, Taoyuan 333, Taiwan
- ⁵ Department of Neurosurgery, Chang Gung Memorial Hospital, Linkou, Taoyuan 333, Taiwan
- ⁶ Artificial Intelligence Research Center, Chang-Gung University, Taoyuan 333, Taiwan
- ⁷ Department of Materials Engineering, Ming-Chi University of Technology, New Taipei City 243, Taiwan
- ⁸ Department of Nephrology, Chang Gung Memorial Hospital, Linkou, Taoyuan 333, Taiwan
- * Correspondence: cslai@mail.cgu.edu.tw; Tel.: +886-3-2118800 (ext. 5786); Fax: +886-3-2118507

Abstract: To evaluate point-of-care testing (POCT) for the potential early detection of biomarkers of Parkinson's disease, a systematic investigation of portable and low-cost platforms is performed based on the Proton-enzyme-linked immunosorbent assay (Proton-ELISA) methodology. The detection of the α -synuclein antigen was first presented by biotin-relative linkers, and glucose substrate solution was first performed with a systematic experimental design to optimize the sensing results. All materials in this study are commercially available. Three different experiments with the partitional check were performed to investigate the Proton-ELISA platform, including proton catalyzed efficiency, blocking efficiency, and full Proton-ELISA procedure. The response time was selected as 15 min by the time-dependent curves of a full reaction. The limit of detection of conventional ELISA kits is 0.169 ng/mL, which is much lower than the Proton-ELISA results. The final response of the full Proton-ELISA procedure to pH changes was approximately 0.60 and 0.12 for α -synuclein antigen concentrations of 100 ng/mL and 4 ng/mL, respectively. With the partitional check, pH changes of pure glucose substrate and conjugated oxidase and interference of the nonspecific binding are 1.7 and 0.04, respectively. The lower pH changes far from the partitional check results can be concluded for the properties of glucose oxidase conjugation, including the isoelectric point and binding affinity modification by the testing environment. This preliminary guideline can be used as a lesson learnt to speed up following studies of the evaluation and optimization of other antigen detection. Therefore, Proton-ELISA can be suggested for some special applications with the help of custom-designed conjugation in the environment with less degradation or interference and a proper detection concentration range.

Keywords: α -synuclein; avidin; glucose; protein; Proton-ELISA



Citation: Yang, C.-M.; Chang, J.-Y.; Chen, M.-Y.; Lai, C.-S. A Systematic Study and Potential Limitations of Proton-ELISA Platform for α -Synuclein Antigen Detection. *Chemosensors* **2022**, *10*, 5. <https://doi.org/10.3390/chemosensors10010005>

Academic Editor: Takahiro Arakawa

Received: 5 November 2021

Accepted: 21 December 2021

Published: 24 December 2021

Publisher's Note: MDPI stays neutral with regard to jurisdictional claims in published maps and institutional affiliations.



Copyright: © 2021 by the authors. Licensee MDPI, Basel, Switzerland. This article is an open access article distributed under the terms and conditions of the Creative Commons Attribution (CC BY) license (<https://creativecommons.org/licenses/by/4.0/>).

1. Introduction

For a better quality of life for more populations around the world, a facile, rapidly detectable, affordable, and portable platform for the quantitative detection of target species in clinical analyses and medical diagnostics is desirable in point-of-care testing (POCT) to replace conventional laboratory-based testing [1–4]. For example, Parkinson's disease is currently a high-impact neurodegeneration disease. The impact ratio in elderly people (e.g., >65 years old) is 2–3% and increases with age [5,6]. The cost of treatments or health care can increase dramatically once the progression becomes more serious. Based on reported data, the total number of Parkinson's disease patients in the United States was approximately 1 million in 2017, and the total economic burden was USD 51.9 billion [7]. In Europe, there are approximately 1.4 million Parkinson's disease patients, and the average

annual cost per patient in 2016 was between EUR 5240 and 19,640 [8]. Based on neurodegeneration, the progression of Parkinson's disease can be classified by Hoehn and Yahr's Scale into five stages [9]. When a large number of substantia nigra striatal dopaminergic neurons have been destroyed, major symptoms, including tremor, muscle stiffness, drooping posture, drooping, difficulty walking, and autonomic symptoms, will appear [10]. There is still a lack of treatment strategies to completely slow down or prevent the progression of PD. In the early stage of PD, it is common to replace or enhance existing dopamine to treat symptoms. However, all current interventions have limited therapeutic benefits for disease progression because the damage may have been developing for a while, and 60% to 80% of the DA neurons in the substantia nigra are lost before symptoms appear [11]. Therefore, substantia nigra loss can be reduced with an improved healing quality if the diagnosis can be precisely performed at the early stage [10]. A rapid screening tool with an affordable price for Parkinson's disease is required. Biomarkers related to Parkinson's disease include tau [12], α -synuclein [13], and beta-amyloid [14] proteins in cerebral spinal fluid (CSF). To meet the requirement for rapid screening, human blood is preferred over CSF owing to its availability. The concentration of these proteins can be 10- to 100-fold lower in blood than in CSF [15]. Therefore, to achieve highly precise detection in blood for POCT, the limit of detection must be further improved. To date, the ELISA has been well accepted as the most commonly used method for testing real samples [4,16]. ELISA can be considered a gold standard protein detection technology due to its high sensitivity, stability, and specificity, and wide applicability [16]. However, due to its constraints in the limit of detection (e.g., from $\mu\text{g/mL}$ to ng/mL), high cost of instrumentation (e.g., color reader for the reaction between enzymes and targets) and nonportability (e.g., large volume and shielding required in signal readout), new technologies have been proposed to overcome the limitations of conventional ELISA from the basis of the colorimetric readout mode, such as electrochemical- and electronic-based readout modes [17–19], or an enhanced signal provided by microscopic beads (e.g., single-molecule array, SiMoA) [20]. Furthermore, Proton-ELISA with good sensitivity and compatibility with field-effect sensors provides a potential candidate for POCT applications [21]. In this study, a new study systematically investigating the Proton-ELISA platform for the detection of α -synuclein is first presented. Time-dependent response and biotin-relative linkers were performed to find an optimized procedure. In addition, the results of conventional ELISA are also discussed.

2. Materials and Methods

2.1. Materials

Detailed information on all materials used in the work is listed in the following section. Glucose, $\text{FeSO}_4 \cdot 7\text{H}_2\text{O}$, bovine serum albumins (BSA) and phosphate buffered saline tablets (PBS) were purchased from Sigma–Aldrich, Merck Co., Darmstadt, Germany. Superblock™ Tween-20 Blocking Buffer (TBS) was purchased from Thermo Fisher Scientific, Waltham, MA, USA. Potassium chloride (KCl) solution at a concentration of 3 M and 96% H_2SO_4 (stop solution) was purchased from Merck Co., Germany. An alpha-synuclein (α -synuclein) ELISA kit including horseradish peroxidase (HRP) and tetramethylbenzidine (TMB) was purchased from R&D, USA. The washing solution was prepared as PBS solution with 0.05% Tween-20 solution added to PBST solution purchased from Sigma–Aldrich. Avidin-glucose oxidase (avidin-GOx) was purchased from ROCKLAND, USA. Streptavidin-glucose oxidase (streptavidin-GOx) was purchased from Fitzgerald, USA. The response signal change of Proton-ELISA was measured by a pH meter (LAQUAtwin pH-22, HORIBA Co., Kyoto, Japan). The deionized (DI) water used in all experiments was purified by a Milli-Q water system (Merck Co., Germany).

2.2. Functionalization of 96-Well Plates with Antibodies

To investigate the Proton-ELISA protocol in detail, the process flow was designed to divide into four subparts (e.g., #1, 2, 3, to 4) to check the function of key steps separately for a better understanding and control of the whole procedure, as shown in Figure 1a.

First, the function of α -synuclein antibodies was verified using the standard ELISA kit protocol to construct the compact structure, as shown in part #1 of Figure 1b. For the surface immobilization of capture antibodies, named the first antibodies (e.g., 1st Ab), the standard solution in the ELISA kit was first diluted to a concentration of 25 ng/mL in a PBS solution. A total of 7 wells of a standard 96-well microplate was immediately injected with this diluted capture antibody solution of 100 μ L to coat α -synuclein antibodies on the surfaces of the wells. The whole plate was sealed and incubated at room temperature overnight. Then, all wells were dried and washed three times with PBST solution as a standard washing step. The processed wells were immersed in 300 μ L of 1% BSA solution and incubated at room temperature for 1 h to achieve the surface blocking step. The same PBST washing step was performed again. For the testing of a seven-point standard curve, the standard α -synuclein antigen solution with a concentration from 0.313 to 20 ng/mL prepared using 2-fold serial dilutions in 1% BSA solution was added into 7 wells in sequence, which were incubated at room temperature for 2 h following a standard washing step. One hundred microliters of the detecting antibody solution, named the secondary antibodies (e.g., 2nd Ab), was added to each well and incubated at room temperature for 2 h following a standard washing step. Then, 100 μ L of the working solution of streptavidin-conjugated HRP was added for the fluorescence reaction. To avoid the influence of room illumination, the whole plate was covered with aluminum foil and incubated for 20 min at room temperature. Then, a substrate solution (e.g., a 1:1 mixture of H_2O_2 and tetramethylbenzidine, TMB) of 100 μ L was added to each well. Finally, 50 μ L stop solution (e.g., H_2SO_4) was added to each well. After the whole modification of each well, the optical density (O.D.) of each well was immediately measured with an ELISA reader (SpectraMax M5, Molecular Devices, San Jose, CA, USA.) according to the difference between the fluorescence intensity at a wavelength of 540 nm and the background intensity under excitation illumination at a wavelength of 450 nm. The O.D. value of each concentration of α -synuclein antigen can be used to plot the calibration curve of these ELISA measurements with these commercial kits.

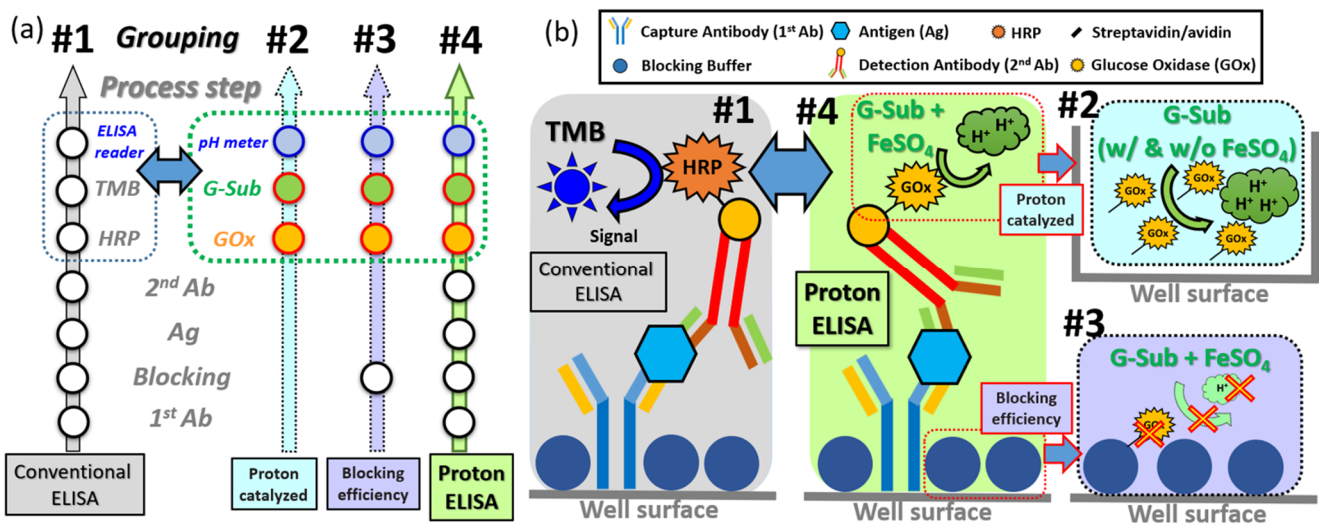


Figure 1. (a) Process flow design and (b) its schematic plot for ELISA, Proton-ELISA and the partitional experiments from part #1 to part #4.

2.3. Proton-Catalyzed Reaction between G-Sub and GOx

In the second experimental part, to confirm the proton-catalyzed reactions between GOx and glucose substrate solution (G-Sub), different GOx-conjugated species and $FeSO_4$ solution were chosen for investigation. The process flow of this experiment and a schematic plot of the final response are shown in part #2, as marked in Figure 1a,b. The avidin or streptavidin conjugated with GOx was used as the biotin for the detected antibody in the procedure of a mixture of G-sub solutions as the experimental group for comparison.

To confirm the reaction efficiency and time response between the GOx and the G-Sub, a real-time experiment of pH value changing was performed to check the pH value per minute first. On the other hand, a solution of 1.5 mL of GOx conjugated with avidin or streptavidin at 0.5 $\mu\text{g}/\text{mL}$ was directly mixed with G-Sub at 1.5 mL for 15 min to check the total response of pH changes (e.g., end-point response) as two distinguished groups. In the meantime, FeSO_4 solution was also added to the G-Sub solution to enhance the generation of protons. The reaction mechanism is presented in Figure S1. Glucose solution was generally composed of 63.6% β -D-glucose and 36.4% α -D-glucose. Glucose oxidase in the presence of O_2 can specifically react with β -D-glucose to generate D-gluconate-1,5-lactone and H_2O_2 . It oxidizes all glucose and can be fully oxidized because the dynamic balance between α - and β -D-glucose-induced β -D-glucose is automatically pushed to the β side when consumed in the reaction [22]. With the help of H_2O , D-gluconate-1,5-lactone can be hydrolyzed to gluconic acid following an increase in the proton concentration in the solution [23]. The FeSO_4 solution can be used to react with the byproduct H_2O_2 to generate more H_2O for the generation of gluconic acid and proton response.

To further enhance the proton signal, the byproduct of hydrogen peroxide (H_2O_2) released by the GOx-catalyzed reaction is coupled with iron(II) sulfate (FeSO_4) to generate additional protons in the solution. The mixture of H_2O_2 and FeSO_4 is called Fenton's reagent [24]. When iron(II) reacted with H_2O_2 to produce H_2O , the reaction formula was pushed to the right, and more gluconic acid was generated. It is also worth noting that the reagents (glucose and FeSO_4) used in the H-ELISA system are low-cost, easy to obtain, and stable at room temperature. The higher the pH change, the higher the sensitivity, which is advantageous in the implementation of the measurement [21].

2.4. GOx Adhesion Check in Different Blocking Buffer Conditions

Nonspecific adhesion is always a critical issue to verify in immunoassays, as it could cause a small signal-to-noise ratio and high interference in real measurements. There is a potential risk that GOx attaches to the well but not to the immobilized detection antibodies without an effective blocking layer on the well surface. To check this concern, BSA or protein-free buffer was used to coat the surface of the well as the blocking layer, and the binding affinity of two different conjugated GOx was verified by the pH change with G-Sub afterward. The process flow and schematic plot of this experiment are shown in part #3, as marked in Figure 1a,b. BSA solutions of 300 μL with different concentrations (e.g., 0.25, 0.5, and 1%), which functioned as the blocking layer, were first added to attach to the well surface with incubation at room temperature for 1 h. Then, 2.5 $\mu\text{g}/\text{mL}$ avidin or streptavidin-conjugated GOx was added and incubated for 30 min at room temperature for binding between BSA and avidin or streptavidin. Next, each well was washed with PBST and 25 mM KCl solution three times to remove all nonbinding species. G-Sub with FeSO_4 solution was added and incubated at room temperature, followed by measurement with a droplet on a pH meter to confirm the response between the BSA blocking layer and conjugated GOx. A pH meter was calibrated with pH 7 and pH 4 in advance to measure the pH after the whole response. Once GOx was bound to the blocking layer, the pH value clearly decreased, which was attributed to the reaction between G-sub and GOx. The smaller the pH changes are, the less binding there is between the BSA blocking layer and conjugated GOx, which is preferred as an acceptable blocking process.

2.5. Process and Measurement of Proton-ELISA

To check the compact Proton-ELISA response, proton generation has to be designed to replace the fluorescence reaction in part #1 in a separate experiment. The process flow and schematic plot of this specific experiment are shown in part #4, as marked in Figure 1a,b. The same procedures, including capture antibody immobilization, surface blocking, and α -synuclein antigen binding, were performed, and then working wells were coated with detection antibody solution (e.g., 25 ng/mL). The α -synuclein antigen concentrations prepared as 0, 4, 20 and 100 ng/mL were used to check the calibration curve

of proton-ELISA measurements. To study the affinity of the two different linkers to GOx, 0.5 $\mu\text{g}/\text{mL}$ GOx conjugated with avidin or streptavidin in 25 mM potassium chloride (KCl) solution was added to bind with detecting antibodies. The incubation for 30 min at room temperature was used to check the final response. Next, all wells were cleaned with the standard washing step, and then a 25 mM KCl wash was used to remove the potential residual PBST, which might interfere with the pH detection in the following step. The pH change with different washing solution for the reaction between GOx and G-sub is shown in Figure S2. The buffer effect of PBST residue can be clearly reduced by the KCl wash. The enzyme-based substrate including G-Sub and FeSO_4 solution (e.g., 6 mg/mL glucose in 25 mM KCl solution and 500 $\mu\text{g}/\text{mL}$ FeSO_4) defined from the conclusion from part #2 was injected into wells and incubated for 5 min at room temperature. This reacted solution was dropped into the pH meter to check the generation of protons as a function of antigen concentration and linkers.

3. Results and Discussion

As with the experimental designs described in Sections 2.2–2.5, the systematic analysis of experimental results will be presented here to provide a scientific research methodology for this Proton-ELISA for α -synuclein antigen detection. Four different parts, defined as #1 to #4, were performed separately to check the applicability of Proton-ELISA. First, the specificity of antibodies bound to antigens is the most important requirement of immune assays. The commercial human alpha-synuclein ELISA kit was selected to check the standard protocol in part #1. As shown in Figure 2, the O.D. values of different concentrations of α -synuclein antigen measured by the ELISA reader could be fitted as a standard four parameter logistic (4PL) curve, which is a regression model often applied to ELISA analysis [25]. Strong evidence can be provided for the correct setup of this standard protocol with a commercial kit. This behaviour results from the higher concentration of α -synuclein antigen, the higher concentration of HRP, and subsequent TMB action. After the stopper solution was added, the response was amplified approximately 3-fold and produced a yellow colour, which could be detected by the ELISA reader. Based on this characteristic, the potential LOD is approximately 0.169 ng/mL, which can be proof of the specificity and sensitivity of this commercial kit and the relative antigens and antibodies.

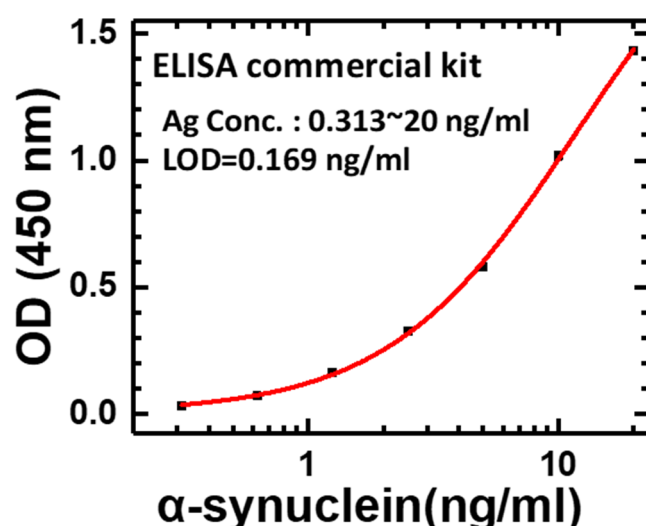


Figure 2. OD value of a calibration curve with different concentrations of α -synuclein antigen measured by conventional ELISA.

To verify the real response of pH changes generated by the reaction between GOx and glucose, pH measurements were performed continuously for 30 min. The time-dependent response of pH changes can be collected to define a reliable reaction time. As shown

in Figure 3, the gradual pH increases with time and can be clearly seen in two different species—avidin- or streptavidin-conjugated GOx (abbreviated as “AG” or “SAG” in Figure 3, respectively). The pH change of the AG group was faster and higher than that of the SAG group. The response time, calculated as the time for 90% of the total response, was approximately 10 and 22 min for the AG and SAG groups, respectively. To have an acceptable response time to compare both reactions, 15 min (e.g., average value between two reactions) was selected as a fixed response time to check the pH changes for the following experimental groups.

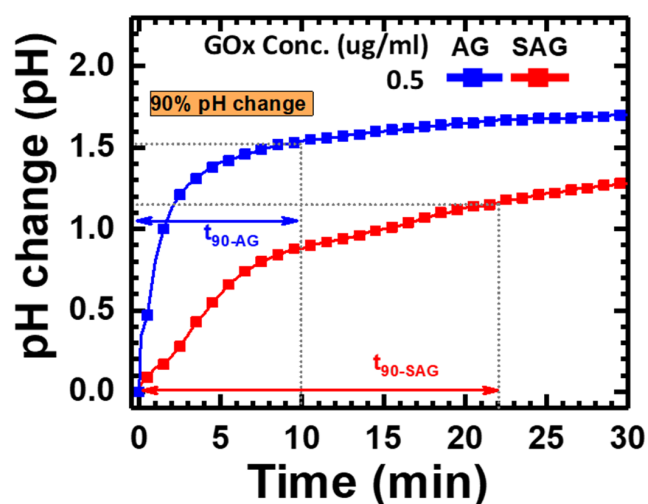


Figure 3. Time-dependent pH changes generated by avidin-conjugated or streptavidin-conjugated GOx at a concentration of 0.5 $\mu\text{g}/\text{mL}$ in part #2 of the experiment.

Next, the experiments are designed for the reaction between glucose concentration and different conjugated GOx to maximize the total response in the pure reaction without interference from other antibodies, antigens, and relative processes. To check the response of pH changes, five glucose concentrations, including 0.005, 0.02, 0.1, 0.5, and 2.5 $\mu\text{g}/\text{mL}$, were applied to react with two different species, including avidin- or streptavidin-conjugated GOx (e.g., “AG” or “SAG” group). In the meantime, adding FeSO_4 solution as an extra catalyst was applied as an enhanced factor for a high pH response, as mentioned in Sections 2 and 3. After adding G-sub of 1.5 mL after 15 min, the pH value of each group was measured as the end-point detection for the final response. As shown in Figure 4, the pH change increased with GOx concentration in all four groups but gradually saturated at concentrations higher than 0.5 $\mu\text{g}/\text{mL}$, which can be explained by the maximum reaction limited by the total glucose concentration in G-sub. At a GOx concentration of 0.5 $\mu\text{g}/\text{mL}$, adding FeSO_4 solution provided 3.47-fold and 5.67-fold pH changes for avidin- and streptavidin-conjugated GOx, respectively. On the other hand, pH changes were higher in the group with avidin-conjugated GOx, which could result from less activity of GOx after conjugation with streptavidin. In the group with a GOx concentration of 0.5 $\mu\text{g}/\text{mL}$ and FeSO_4 addition, avidin-conjugated GOx (e.g., “AG” group) had 59% higher pH changes than streptavidin-conjugated GOx (e.g., “SAG” group). This behaviour could be determined by the natural properties of these two commercial products. The optimized condition for the highest pH change of 1.7 is found in the group of avidin-conjugated GOx with a concentration of 0.5 $\mu\text{g}/\text{mL}$ added to FeSO_4 , which could be helpful for a wide antigen detection range and limit of detection.

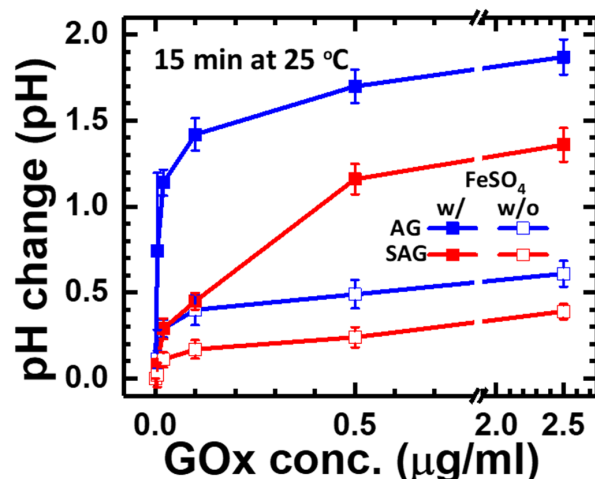


Figure 4. Endpoint pH change with different concentrations of avidin-conjugated or streptavidin-conjugated GOx and adding FeSO₄ solution after 15 min of reaction in part #2.

Before the compact Proton-ELISA experiment, the interference between blocking protein and AG and SAG should be checked for nonspecific binding on the surface of wells by means of the process design of part #3. In general, the binding ability between AG or SAG to blocking proteins should be very low. Therefore, the following pH changes generated by the binding AG or SAG reacted with G-sub should be very small. As shown in Figure 5, groups with different blocking protein conditions all have pH changes less than 0.12, which can be considered the interference of nonspecific binding of reaction wells. Therefore, the lowest pH change of AG and SAG was observed for the group with protein-free blocking, which can be suggested as the standard blocking process for Proton-ELISA. The total pH changes of the signal (e.g., conjugated GOx with a concentration of 0.5 μg/mL added to FeSO₄) shown in Figure 4 divided by the total pH changes of interference (e.g., the same conjugated GOx concentration with protein-free blocking) shown in Figure 5 for AG- and SAG-conjugated GOx can be calculated as the signal-to-noise ratio (SNR). The SNRs of AG- and SAG-conjugated GOx are 43 and 38, respectively. Therefore, avidin-conjugated GOx with a high SNR can be expected to have a better response.

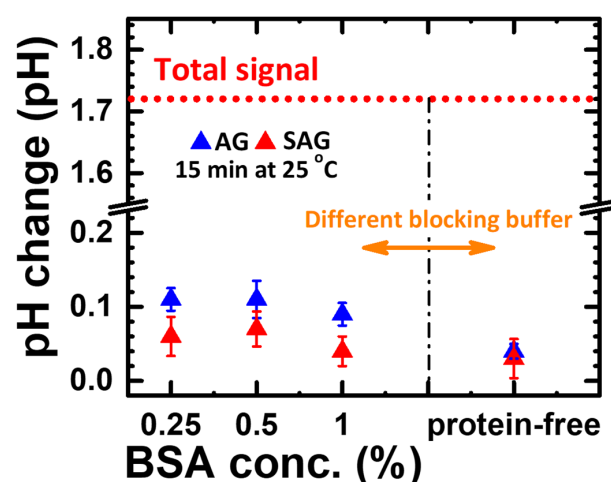


Figure 5. Endpoint pH change generated by nonspecific interaction of different blocking buffer solutions treated on the well surfaces in the experiment of part #3.

Based on the conclusions of parts #1 to #3, the SOP with confirmed specific binding between the antibody and antigen, less interference, and a high pH response can be confirmed by partitional procedures. The response time was 15 min. For the total proton-ELISA in the detection of the α -synuclein antigen, part #4 was performed with four different

concentrations (e.g., 0, 4, 20, 100 ng/mL) of the α -synuclein antigen for the AG and SAG groups. As shown in Figure 6, high pH changes can be found in the AG group compared to the SAG group, which meets our expectation based on the conclusion of part #2. The main reason could be concluded that streptavidin generally has an acid isoelectric point (e.g., PI = 5) [26]. When it is added to a G-Sub environment with a pH of 5, its solubility will be decreased, which makes the protein easily aggregate and even precipitate. This is because the net charge on the protein molecules gradually tends to zero, and the mutual repulsion between the protein molecules decreases; thus, the activity of the enzyme is affected [27]. In contrast, avidin has a relatively alkaline isoelectric point (e.g., PI = 10) [28], and its high solubility does not easily cause aggregation and precipitation. In addition, avidin has D-glucosamine [28], which can be oxidized by GOx to form D-gluconic acid and increase the number of protons in the solution [29]. On the other hand, the affinity of streptavidin for binding biotin is verified to be only 50~70% of the maximum biotin binding capacity of avidin [29], which also impacts the efficiency of GOx binding to the second Ab. Even so, the total pH change for an α -synuclein concentration of 100 ng/mL in the AG group was approximately 0.60, which was much lower than the full response of pH changes of 1.7, as shown in part #2. When the α -synuclein concentration was reduced to 4 ng/mL in the AG group, the pH changed by only 0.12, which is close to the limitation of a pH detection resolution of 0.01. This dramatic reduction ratio of pH changes could lead to a narrow application range in the α -synuclein concentration no lower than the level of a few ng/mL. We concluded that the affinity between AG and GOx can be inhibited by the α -synuclein antigen and follow a lower pH response. A schematic plot to illustrate the whole response according to pH changes in the partitioned investigation is shown in Figure 7. Although Proton-ELISA could have high application potential, the final response and application range could also be limited by the reaction between all species and targets, especially enzyme-based reactions [22]. Because the current reagents are all purchased from commercial products, optimization for a high pH response cannot be easily performed. Current protocol and results are not suitable to test clinical samples from patients with Parkinson's disease. Based on this systematic analysis of all experiments, the Proton-ELISA platform with an inferior performance compared to conventional ELISA can be suggested only with custom-designed reagents and proper reactions with optimization. The application range and resolution of target detection could be limited. Some potential applications in species with high concentrations or rapid screening of a clear cut-off point could be investigated based on this Proton-ELISA platform due to the low cost and simple readout instrument.

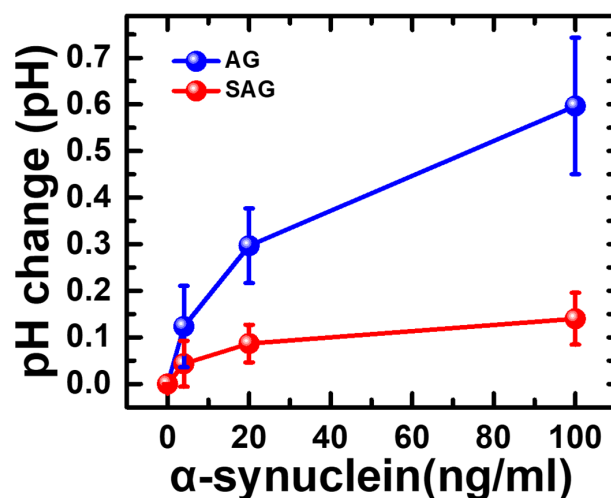


Figure 6. Endpoint pH change generated by the whole Proton-ELISA process for different concentrations of α -synuclein antigen and two different conjugated GOx in part #4 of the experiment.

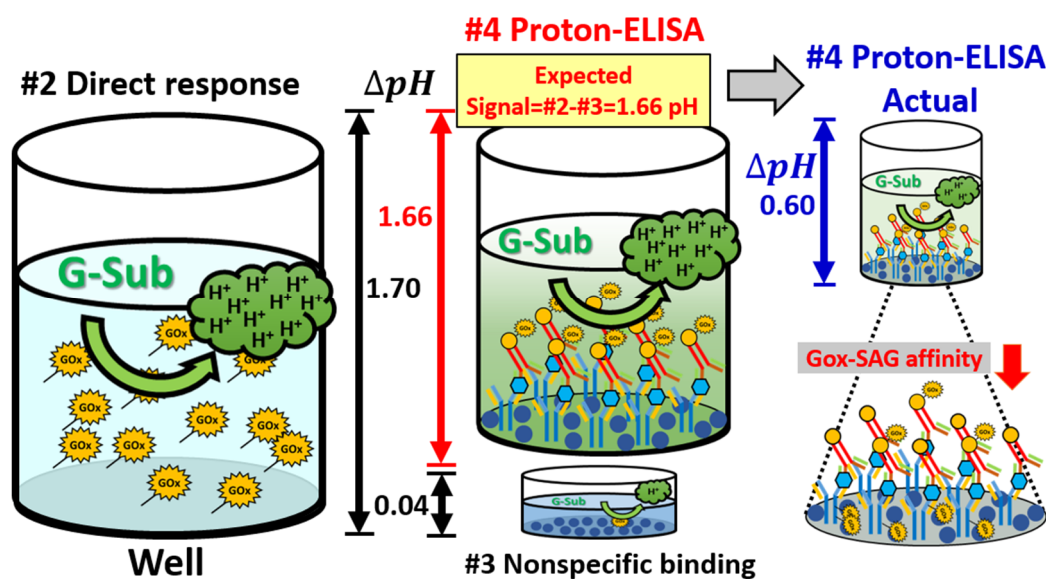


Figure 7. Schematic plot of the detailed mechanism to explain the resulting differences between partitional check and full Proton-ELISA.

4. Conclusions

To check the potential of the nonELISA platform, the Proton-ELISA platform was selected for the detection of the α -synuclein antigen. The reaction between the α -synuclein antibody and antigen from commercial kits was proven first by conventional ELISA. A partitional check of the Proton-ELISA standard procedure was carried out with two major loops: the reaction between glucose substrate solution and avidin- or streptavidin-conjugated glucose oxidase and the nonspecific binding of well surfaces. The pH changes of the pure response of the glucose substrate and conjugated oxidase and interference of nonspecific binding are 1.7 and 0.04, respectively. The final response of the full Proton-ELISA procedure to pH changes was approximately 0.60 and 0.12 for α -synuclein antigen concentrations of 100 ng/mL and 4 ng/mL, respectively. This small pH change has a large difference from the partitional check results, which can be concluded for the properties of conjugation of glucose oxidase, including the isoelectric point and binding affinity modification, by the testing environment. Therefore, Proton-ELISA can be suggested for custom-designed conjugation and reactions for applications with less degradation or interference in the proper concentration range.

Supplementary Materials: The following are available online at <https://www.mdpi.com/article/10.3390/chemosensors10010005/s1>, Figure S1: Schematic plot of the reaction of Proton-ELISA with GOx and FeSO₄ solution. Figure S2: The pH change by a different washing process including no wash, PBST only and PBST + KCl washing for Gox and G-sub reaction, which followed the same protocol as Part #2. It can be clearly seen PBST + KCl washing had reduced the buffer residue and its function.

Author Contributions: Conceptualization, C.-M.Y., J.-Y.C. and C.-S.L.; methodology, J.-Y.C. and M.-Y.C.; formal analysis, investigation, data curation, and validation, C.-M.Y., J.-Y.C. and M.-Y.C.; visualization, J.-Y.C. and C.-S.L.; writing—original draft preparation original manuscript writing, C.-M.Y. and C.-S.L.; writing—review and editing, C.-M.Y. and C.-S.L.; supervision, C.-S.L. All authors have read and agreed to the published version of the manuscript.

Funding: This work was funded by Chang Gung Memorial Hospital (at Linkou), Taiwan under contract numbers CMRPD2I0012, CMRPD2K0171, CORPD2J0072-73, Ministry of Science of Technology of Taiwan under contract numbers 108-2221-E-182-060-MY3, 108-2628-E-182-002-MY3, 109-2221-E-182-013-MY3, 110-2221-E-182-043-MY3 and Taiwan Semiconductor Manufacturing Co., Ltd. (TSMC) joint developed project under contract numbers TUP-20210506-2016.

Institutional Review Board Statement: Not applicable.

Informed Consent Statement: Not applicable.

Data Availability Statement: The data presented in this study are available on request from the corresponding authors.

Acknowledgments: The authors appreciate the kind help and suggestions provided by Shih-Fen Huang, Chun-Ren Cheng, Fu-Chun Huang, and Ching-Hui Lin at Taiwan Semiconductor Manufacturing Co., Ltd. (TSMC).

Conflicts of Interest: The authors declare no conflict of interest.

References

1. Tang, Z.; Ma, Z. Multiple functional strategies for amplifying sensitivity of amperometric immunoassay for tumor markers: A review. *Biosens. Bioelectron.* **2017**, *98*, 100–112. [[CrossRef](#)]
2. Liu, J.; Geng, Z.; Fan, Z.; Liu, J.; Chen, H. Point-of-care testing based on smartphone: The current state-of-the-art (2017–2018). *Biosens. Bioelectron.* **2019**, *132*, 17–37. [[CrossRef](#)] [[PubMed](#)]
3. Giannetti, A.; Trono, C.; Porro, G.; Domenici, C.; Puntoni, M.; Baldini, F. Towards an Integrated System as Point-of-Care Device for the Optical Detection of Sepsis Biomarkers. *Chemosensors* **2020**, *8*, 12. [[CrossRef](#)]
4. Younes, N.; Al-Sadeq, D.W.; Al-Jighefee, H.; Younes, S.; Al-Jamal, O.; Daas, H.I.; Nasrallah, G.K. Challenges in laboratory diagnosis of the novel coronavirus SARS-CoV-2. *Viruses* **2020**, *12*, 582. [[CrossRef](#)] [[PubMed](#)]
5. Jankovic, J. Parkinson's disease: Clinical features and diagnosis. *J. Neurol. Neurosurg. Psychiatry* **2008**, *79*, 368–376. [[CrossRef](#)] [[PubMed](#)]
6. Poewe, W.; Seppi, K.; Tanner, C.M.; Halliday, G.M.; Brundin, P.; Volkmann, J.; Lang, A.E. Parkinson disease. *Nat. Rev. Dis. Primers* **2017**, *3*, 1–21. [[CrossRef](#)]
7. Yang, W.; Hamilton, J.L.; Kopil, C.; Beck, J.C.; Tanner, C.M.; Albin, R.L.; Dorsey, E.R.; Dahodwala, N.; Cintina, I.; Hogan, P.; et al. Current and projected future economic burden of Parkinson's disease in the U.S. *NPJ Parkinson's Dis.* **2020**, *6*, 15. [[CrossRef](#)]
8. Kruse, C.; Kretschmer, S.; Lipinski, A.; Verheyen, M.; Mengel, D.; Balzer-Geldsetzer, M.; Lorenzl, S.; Richinger, C.; Schmotz, C.; Tönges, L.; et al. Resource Utilization of Patients with Parkinson's Disease in the Late Stages of the Disease in Germany: Data from the CLaSP Study. *Pharmacoeconomics* **2021**, *39*, 601–615. [[CrossRef](#)]
9. Hoehn, M.M.; Yahr, M.D. Parkinsonism: Onset, progression, and mortality. *Neurology* **1998**, *50*, 318. [[CrossRef](#)]
10. Miller, D.B.; O'Callaghan, J.P. Biomarkers of Parkinson's disease: Present and future. *Metabolism* **2014**, *64*, S40–S46. [[CrossRef](#)]
11. Lang, A.E.; Lozano, A.M. Parkinson's disease. *N. Engl. J. Med.* **1998**, *339*, 1130–1143. [[CrossRef](#)]
12. Compta, Y.; Martí, M.J.; Ibarretxe-Bilbao, N.; Junqué, C.; Valldeoriola, F.; Muñoz, E.; Tolosa, E. Cerebrospinal tau, phospho-tau, and beta-amyloid and neuropsychological functions in Parkinson's disease. *Mov. Disord.* **2009**, *24*, 2203–2210. [[CrossRef](#)] [[PubMed](#)]
13. Stefanis, L. α -Synuclein in Parkinson's disease. *Cold Spring Harb. Perspect. Med.* **2012**, *2*, a009399. [[CrossRef](#)]
14. Lim, E.W.; Aarsland, D.; Ffytche, D.; Taddei, R.N.; van Wamelen, D.J.; Wan, Y.M.; Chaudhuri, K.R. Amyloid- β and Parkinson's disease. *J. Neurol.* **2019**, *266*, 2605–2619. [[CrossRef](#)]
15. Shi, M.; Kovac, A.; Korff, A.; Cook, T.J.; Gingham, C.; Bullock, K.M.; Zhang, J. CNS tau efflux via exosomes is likely increased in Parkinson's disease but not in Alzheimer's disease. *Alzheimer's Dement.* **2016**, *12*, 1125–1131. [[CrossRef](#)]
16. Bettazzi, F.; Enayati, L.; Sánchez, I.C.; Motaghed, R.; Mascini, M.; Palchetti, I. Electrochemical bioassay for the detection of TNF- α using magnetic beads and disposable screen-printed array of electrodes. *Bioanalysis* **2013**, *5*, 11–19. [[CrossRef](#)] [[PubMed](#)]
17. Zhang, D.; Li, W.; Ma, Z.; Han, H. Improved ELISA for tumor marker detection using electro-readout-mode based on label triggered degradation of methylene blue. *Biosens. Bioelectron.* **2018**, *126*, 800–805. [[CrossRef](#)] [[PubMed](#)]
18. Wang, Y.; Zhao, G.; Wang, H.; Cao, W.; Du, B.; Wei, Q. Sandwich-type electrochemical immunoassay based on $\text{Co}_3\text{O}_4/\text{MnO}_2$ -thionine and pseudo-ELISA method toward sensitive detection of alpha fetoprotein. *Biosens. Bioelectron.* **2018**, *106*, 179–185. [[CrossRef](#)] [[PubMed](#)]
19. Arya, S.K.; Estrela, P. Electrochemical ELISA-based platform for bladder cancer protein biomarker detection in urine. *Biosens. Bioelectron.* **2018**, *117*, 620–627. [[CrossRef](#)]
20. Rissin, D.M.; Kan, C.W.; Campbell, T.G.; Howes, S.C.; Fournier, D.R.; Song, L.; Piech, T.; Patel, P.P.; Chang, L.; Rivnak, A.J.; et al. Single-molecule enzyme-linked immunosorbent assay detects serum proteins at subfemtomolar concentrations. *Nat. Biotechnol.* **2010**, *28*, 595–599. [[CrossRef](#)]
21. Juang, D.S.; Lin, C.-H.; Huo, Y.-R.; Tang, C.-Y.; Cheng, C.-R.; Wu, H.-S.; Huang, S.-F.; Kalnitsky, A.; Lin, C.-C. Proton-ELISA: Electrochemical immunoassay on a dual-gated ISFET array. *Biosens. Bioelectron.* **2018**, *117*, 175–182. [[CrossRef](#)]
22. Raba, J.; Mottola, H.A. Glucose Oxidase as an Analytical Reagent. *Crit. Rev. Anal. Chem.* **1995**, *25*, 1–42. [[CrossRef](#)]
23. Leskovac, V.; Trivić, S.; Wohlfahrt, G.; Kandrač, J.; Peričin, D. Glucose oxidase from *Aspergillus niger*: The mechanism of action with molecular oxygen, quinones, and one-electron acceptors. *Int. J. Biochem. Cell Biol.* **2005**, *37*, 731–750. [[CrossRef](#)]
24. Walling, C. Fenton's reagent revisited. *Acc. Chem. Res.* **1975**, *8*, 125–131. [[CrossRef](#)]

25. Masdor, N.A. Determination of the detection limit using the four-parameter logistic model for the double-antibody sandwich ELISA for the rapid detection of *Bacillus cereus* in food. *J. Environ. Microbiol. Toxicol.* **2017**, *5*, 12–13.
26. Green, N.M. [5] Avidin and streptavidin. *Methods Enzymol.* **1990**, *184*, 51–67. [[CrossRef](#)]
27. Golovanov, A.P.; Hautbergue, G.M.; Wilson, S.A.; Lian, L.-Y. A Simple Method for Improving Protein Solubility and Long-Term Stability. *J. Am. Chem. Soc.* **2004**, *126*, 8933–8939. [[CrossRef](#)]
28. Green, N.M. Avidin. In *Advances in Protein Chemistry*; Academic Press: Cambridge, MA, USA, 1975; Volume 29, pp. 85–133.
29. Pezzotti, F.; Therisod, H.; Therisod, M. Enzymatic synthesis of D-glucosaminic acid from D-glucosamine. *Carbohydr. Res.* **2005**, *340*, 139–141. [[CrossRef](#)] [[PubMed](#)]